

# Growth and Survival Mechanisms Associated with Perineural Invasion in Prostate Cancer

Gustavo E. Ayala,<sup>1,2</sup> Hong Dai,<sup>1</sup> Michael Ittmann,<sup>1</sup> Rile Li,<sup>1</sup> Michael Powell,<sup>1</sup> Anna Frolov,<sup>2</sup> Thomas M. Wheeler,<sup>1,2</sup> Timothy C. Thompson,<sup>2,3</sup> and David Rowley<sup>3</sup>

Departments of <sup>1</sup>Pathology, <sup>2</sup>Urology, and <sup>3</sup>Molecular and Cellular Biology, Baylor College of Medicine, Houston, Texas

## ABSTRACT

Perineural invasion (PNI) is the major mechanism of prostate cancer spread outside the prostate. Apoptotic and proliferation indices were determined in PNI cells using the PNI *in vitro* model and human PNI in tissue microarrays. RNA was extracted from the PNI model and controls and evaluated by cDNA microarray analysis. Differential expression of candidate genes was confirmed by real-time quantitative PCR, fluorescence, and immunohistochemistry using tissue microarrays. Genistein and BAY 11-7085 were added to the supernatant of cocultures and controls in microchamber cultures. The significance of nuclear factor  $\kappa$ B (NF $\kappa$ B) nuclear translocation in human PNI was analyzed using Kaplan-Meier analysis. An increase in proliferation and a decrease in apoptosis were observed in human PNI cells and the PNI model as compared with controls. Three of 15 genes up-regulated in the cDNA microarray were involved in the apoptosis signaling pathway (NF $\kappa$ B), and its downstream targets defender against cell death 1 and PIM-2. The increase was corroborated by real-time quantitative PCR and immunofluorescence. NF $\kappa$ B nuclear translocation was seen in the *in vitro* model and human tissues, where strong nuclear expression was associated with a decrease in recurrence-free survival. Addition of genistein and BAY 11-7085 resulted in a decrease in NF $\kappa$ B, PIM-2 and defender against cell death 1 as well as a reversal of the inhibition of apoptosis. This is the first description of a biological mechanism and functional significance of PNI. Cancer cells in a perineural location acquire a survival and growth advantage using a NF $\kappa$ B survival pathway. Targeting PNI might help detain local spread of the tumor and influence survival.

## INTRODUCTION

Perineural invasion (PNI) is the process by which cancer cells wrap around nerves. It was first described by Ernst in 1905 (1). It is seen most frequently in certain types of cancer such as prostate, bile duct, and pancreatic carcinomas as well as head and neck cancers. Because of their predilection for nerves, these cancers are known as “neurotropic cancers.” For approximately 60 years, researchers believed that PNI was an expression of tumors cells traveling through lymphatic vessels within the perineural space. Rodin *et al.* (2) demonstrated that the perineural space was devoid of lymphatic vessels and, in the absence of a biological explanation, concluded that PNI was a purely physical phenomenon. Cancer cells found a pre-established dissemination route of “least resistance” in the perineural space (2).

Prostate cancer currently is the most common noncutaneous malignancy and the second leading cause of cancer death in American men (3). Mortality in prostate cancer patients is generally attributable to extracapsular spread, which often results in treatment failure and is associated with poor prognosis (4). Perineural invasion is reported in 85% of prostate cancer patients. More importantly, at least 50% of

cases involving extracapsular extension occurred by spread of the cancer within the perineural spaces (5). Accordingly, current theories suggest that PNI is a key process for extraprostatic spread in prostate cancer.

A previous study with a small number of cases has reported a decrease in apoptotic rate and increased proliferation in cancer cells in a perineural location as compared with cells away from the nerve (6). However, little is understood about the specific mechanisms that regulate PNI in prostate cancer. We are aware of no new biological studies involving PNI for the last 35 years.

It is likely that a set of key signaling pathways mediate interactions between nerves and cancer cells, which result in PNI and spread of prostate cancer beyond the gland. To address specific mechanisms, we recently developed the PNI *in vitro* model of PNI (7). This model showed that specific interactions existed between prostate cancer cells and nerves, which led to costimulation of growth and PNI *in vitro*. As we reported previously, DU-145 cells and ganglion neuron neurites migrate toward each other, and the cancer cells contact the nerves and migrate in the perineural sheath (7). Accordingly, the PNI *in vitro* model is useful in permitting the analysis of specific signaling mechanisms that regulate changes in cell proliferation and survival associated with PNI in prostate cancer. To understand mechanisms involved in PNI, we used the PNI *in vitro* model and human prostate cancer tissue arrays to identify and assess specific factors that might regulate this biology. We report here that prostate cancer cells in a perineural position exhibit a significantly reduced rate of apoptosis and an increased rate of proliferation. Furthermore, we show that up-regulation of nuclear factor  $\kappa$ B (NF $\kappa$ B) and its downstream targets PIM-2 and defender against cell death 1 (DAD-1), all components involved in antiapoptosis signaling cascades, is associated with prostate cancer cells in PNI and most likely regulates the inhibition of apoptosis.

## MATERIALS AND METHODS

**Perineural Invasion *In vitro* System.** The PNI *in vitro* coculture model consists of human prostate cancer cells (DU-145) and mouse ganglia/nerves embedded in Matrigel following the conditions we have published previously (7). Briefly, dorsal root ganglia/nerves (DRG) from 4- to 7-week-old C57BL/6 mice were removed surgically and cocultured with DU-145 cells in EHS Matrigel (Becton Dickinson, Bedford, MA). Cultures were grown in RPMI 1640 medium (GIBCO, Grand Island, NY) containing 10% heat-inactivated fetal bovine serum (GIBCO) in a humidified atmosphere of 5% CO<sub>2</sub>. DU-145 alone and DRG alone were cultured as controls. Between days 9 and 11, some cultures were fixed (3.7% buffered formalin) and processed for immunohistochemistry. Identical cultures were processed for RNA extraction. Residual conditioned media (48 hours) from all cultures were used fresh in the microchamber system.

**Microchamber System.** DU-145 human prostate carcinoma cells were obtained from American Type Culture Collection (Manassas, VA) and cultured in RPMI 1640 supplemented with fetal bovine serum (10%), penicillin (100 units/ml), and streptomycin (100  $\mu$ g/ml; Sigma, St. Louis, MO). They were maintained at 37°C in a humidified atmosphere of 5% CO<sub>2</sub>. DU-145 cells were cultured in microchamber culture slides (VWR) as monolayer adherent cells for 11 days to approximately 70–80% confluence. The cultures were then switched to 50% fresh medium and 50% conditioned medium transferred from

Received 3/8/04; revised 6/24/04; accepted 7/9/04.

**Grant support:** Supported by National Institutes of Health Specialized Programs of Research Excellence CA58204 and Department of Defense PC 991371.

The costs of publication of this article were defrayed in part by the payment of page charges. This article must therefore be hereby marked *advertisement* in accordance with 18 U.S.C. Section 1734 solely to indicate this fact.

**Requests for reprints:** Gustavo E. Ayala, Department of Pathology, Baylor College of Medicine, One Baylor Plaza, Houston, TX 77030. Phone: 713-394-6487; Fax: 713-793-1603; E-mail: gayala@bcm.tmc.edu.

©2004 American Association for Cancer Research.

# Report Documentation Page

*Form Approved*  
*OMB No. 0704-0188*

Public reporting burden for the collection of information is estimated to average 1 hour per response, including the time for reviewing instructions, searching existing data sources, gathering and maintaining the data needed, and completing and reviewing the collection of information. Send comments regarding this burden estimate or any other aspect of this collection of information, including suggestions for reducing this burden, to Washington Headquarters Services, Directorate for Information Operations and Reports, 1215 Jefferson Davis Highway, Suite 1204, Arlington VA 22202-4302. Respondents should be aware that notwithstanding any other provision of law, no person shall be subject to a penalty for failing to comply with a collection of information if it does not display a currently valid OMB control number.

1. REPORT DATE <b>SEP 2004</b>	2. REPORT TYPE	3. DATES COVERED <b>00-00-2004 to 00-00-2004</b>			
4. TITLE AND SUBTITLE <b>Growth and Survival Mechanisms Associated with Perineural Invasion in Prostate Cancer</b>		5a. CONTRACT NUMBER			
		5b. GRANT NUMBER			
		5c. PROGRAM ELEMENT NUMBER			
6. AUTHOR(S)		5d. PROJECT NUMBER			
		5e. TASK NUMBER			
		5f. WORK UNIT NUMBER			
7. PERFORMING ORGANIZATION NAME(S) AND ADDRESS(ES) <b>Baylor College of Medicine, Department of Pathology, Houston, TX, 77030</b>		8. PERFORMING ORGANIZATION REPORT NUMBER			
9. SPONSORING/MONITORING AGENCY NAME(S) AND ADDRESS(ES)		10. SPONSOR/MONITOR'S ACRONYM(S)			
		11. SPONSOR/MONITOR'S REPORT NUMBER(S)			
12. DISTRIBUTION/AVAILABILITY STATEMENT <b>Approved for public release; distribution unlimited</b>					
13. SUPPLEMENTARY NOTES <b>The original document contains color images.</b>					
14. ABSTRACT					
15. SUBJECT TERMS					
16. SECURITY CLASSIFICATION OF:			17. LIMITATION OF ABSTRACT	18. NUMBER OF PAGES <b>9</b>	19a. NAME OF RESPONSIBLE PERSON
a. REPORT <b>unclassified</b>	b. ABSTRACT <b>unclassified</b>	c. THIS PAGE <b>unclassified</b>			

the PNI coculture model and controls (DU-145 cell growing alone; day 7). Fresh RPMI 1640-based culture medium was also used as a control. Genistein (Sigma) was dissolved in 0.1 mol/L Na<sub>2</sub>CO<sub>3</sub> to make a 10 mmol/L stock solution and added directly to the culture medium at a final concentration of 50 μmol/L. Samples were treated with genistein or vehicle control for 96 hours. All samples were cultured for a total of 10 days and then fixed in 3.7% buffered formaldehyde and processed for *in situ* apoptotic body labeling.

BAY 11-7085 (Calbiochem, La Jolla, CA) was dissolved in dimethyl sulfoxide to make a 10 mmol/L solution and added directly to the culture medium at a final concentration of 10 μmol/L. Samples were treated with BAY 11-7085 or vehicle control also for 96 hours.

**Labeling and Hybridization of cDNA for Microarray Analysis.** Microarray analysis was performed using 30 μg of total RNA. cDNA reverse transcription and fluorescent labeling reactions were carried out using Cy3-labeled nucleotides for control and Cy5-labeled nucleotides for experimental samples. Briefly, cDNA synthesis was initiated by incubating RNA with nonlabeled oligo(dT) primer (1.5 μg; Life Technologies, Inc.) in a 39-μl total volume at 70°C for 10 minutes and chilled on ice. Then, Cy3- and Cy5-labeled dCTPs (Amersham Life Science, Arlington Heights, IL) were added to the appropriate reactions. To each reaction, we added 5× first-strand buffer [12 μl; 250 mmol/L Tris-HCl (pH 8.3), 375 mmol/L KCl, and 15 mmol/L MgCl<sub>2</sub>], unlabeled nucleotide mix (3 μl; 1 mmol/L dATP, dGTP, and dTTP and 0.1 mmol/L dCTP), 0.1 mol/L dithiothreitol (6 μl), 3 μl of Superscript II reverse transcriptase (200 units/μl), and RNase inhibitor (6 μl; 20 units/μl). After incubation at 42°C for 2 h, cDNA was denatured and neutralized by adding 3 μl of 5 mol/L NaOH and incubation at 37°C for 10 minutes, followed by the addition of 15 μl of Tris-HCl (pH 7.5) and 3 μl of 5 mol/L HCl. The mixture of Cy3 and Cy5 reactions was used as probe and purified using Qiagen PCR purification kit (Qiagen, Valencia, CA). The probe was then mixed with an equal amount of ultrahyb hybridization buffer (Ambion, Austin, TX) and denatured by a 2-minute incubation in boiling water to hybridize in Genomic Systems Hybridization station for 4 hours at 42°C against a microarray chip carrying 6,000 cDNAs obtained from Baylor Microarray Core Facility.<sup>4</sup> After hybridization and post-hybridization washes, the slide was scanned immediately in an Axon 4000A dual channel scanner (Axon Instruments, Foster City, CA), and the data were analyzed using the Gene Pix version 3.0 software package (Axon). Genes were considered up- or down-regulated if expression was changed at least 2-fold as compared with the control. Data with low signal intensity, high background, and high variability were eliminated.

**First-Strand cDNA Synthesis.** First-strand cDNA were made from total RNA by using RETROscript First Strand Synthesis Kit (Ambion). One microgram of each RNA sample and control template RNA (Ambion) was heated to 75°C for 3 minutes in nuclease-free water containing 2 μl of random decamers. Two microliters of 10× reverse transcription buffer, 4 μl of 10 mmol/L deoxynucleoside triphosphate mix (10 mmol/L each dATP, dCTP, dGTP, and dTTP), 1 μl of placental RNase inhibitor, and 1 μl of Moloney murine leukemia virus reverse transcriptase (100 units/μl) were added to the sample. Each reaction volume was adjusted to 20 μl by adding nuclease-free water. The reaction mixture was incubated at 44°C for 1 hour, followed by incubation at 92°C for 10 minutes to inactivate the reverse transcriptase.

**Real-Time Quantitative Polymerase Chain Reaction.** The ABI Prism 7000 sequence detection system (Applied Biosystems, Foster City, CA) was used for quantitative PCR analysis using hypoxanthine phosphoribosyltransferase 1 (HPRT1) as endogenous control. All probes (6-FAM dye labeled at the 5' end and a nonfluorescent quencher at the 3' end of the probe) were combined with primers (Assay-on-Design; Applied Biosystems). Validation experiments were performed using 1:2 diluted templates. The log input amount of RNA *versus* ΔCt was generated to demonstrate that the efficiencies of the targets and references were approximately equal. DAD-1, NFκB, PIM-2 (sequences available on request), and HPRT1 genes were amplified in separate wells in duplicate. Reaction conditions included 10 μl of 2× TaqMan Universal Master Mix (with UNG), 1 μl of HPRT1 or target primers and probes mixture, 100 ng of template cDNA (DU-145 alone, PNI coculture, and PNI coculture with genistein), and nuclease-free water to a 96-well reaction plate. The total reaction volume is 20 μl. The TaqMan cycling conditions were as

follows: 2 minutes at 50°C; 10 minutes at 95°C, and 40 cycles of 15 seconds at 95°C followed by 1 minute at 60°C.

Calculation was performed using values of Δ cycle threshold (ΔCt) as the calibrator from DU-145 cells cultured alone or from DU-145 cells cocultured with DRG. For each experimental sample, the Ct of target, normalized to an endogenous reference and relative to a calibrator, is given by:  $2^{-\Delta\Delta Ct}$ .

**Cohort Enrollment and Tissue Microarrays.** More than 4,000 patients underwent radical prostatectomies at one of the Baylor College of Medicine-affiliated institutions and willingly provided tissues (IRB H-1158). A single pathologist (T. M. W.) performed the pathological analysis of the radical prostatectomies. Of these, 226 were used to build tissue microarrays with the manual tissue arrayer (Beecher Instruments Microarray Technology, Silver Spring, MD). Entry criteria included: (a) no preoperative treatment; (b) surgery between 1983 and 1998; (c) prostate cancer present in the surgical specimen and large enough to be cored (2-mm cores) for microarrays; and (d) PNI present and large enough to be cored. A smaller array using tissues from 50 patients was also built.

Whole mount slides were examined under light microscope, and areas of nerves with PNI were marked. Areas of cancer far away from the nerve were also selected [non-PNI (NPNI)]. One tissue cylinder (2 mm) was punched from the PNI area and the NPNI area of each specimen and transferred to an empty recipient paraffin block. The Baylor Institutional Review Board (IRB H-13024) approved this study.

**In situ Labeling of Apoptotic Bodies.** The detection of DNA fragmentation was determined *in situ* by the terminal deoxynucleotidyl transferase-mediated nick end labeling (TUNEL) technique as described previously (8). We used the TACS-XL-diaminobenzidine *in situ* apoptosis kit (Trevigen Inc., Gaithersburg, MD) following the manufacturer's indicator with minor modifications and counterstained with methyl green. The TUNEL assay and immunohistochemistry were performed on the tissue microarray slides and paraffin-embedded sections of PNI coculture and controls. A positive control slide prepared by TACS-nuclease and a specimen known to be positive for apoptotic cells were used as positive controls. Substitution of terminal deoxynucleotidyl transferase with distilled water was used as a negative control.

Apoptotic bodies were counted under a light microscope (×400) equipped with an ocular grid (10,000 μm<sup>2</sup>). The area with highest positive stain was selected for counting. The number of apoptotic bodies was determined in a total of approximately 2,000 prostate cancer cells, normalized to 100 cells, and defined as apoptotic index (AI). At least 10 representative areas without necrosis were selected. Positively stained cells or bodies located in the stroma and lumen were excluded because these apoptotic cells or bodies might have originated from other cell types.

**Immunohistochemistry.** The proliferation rate of prostate cancer cells in human tissues and in the PNI *in vitro* model was determined using the immunoperoxidase method with antibodies against Ki-67 (Santa Cruz Biotechnology, Santa Cruz, CA). Briefly, the slides were deparaffinized and rehydrated in graded ethanol, and antigens were retrieved using steam in 10 mmol/L citrate buffer (pH 6.0) for 30 minutes. The slides were subsequently blocked with blocking protein (DAKO, Carpinteria, CA) for 10 minutes and then incubated with the polyclonal antibody Ki-67 (C-20), for 1 hour at room temperature at a dilution of 1:50. The secondary biotinylated antibody was applied for 30 minutes followed by a 30-minute incubation with streptavidin peroxidase (DAKO LSAB+HRP kit). After rinsing, slides were visualized by diaminobenzidine chromogen solution (DAKO) and counterstained with routine hematoxylin. Positive staining of Ki-67 was confined to the nucleus. The proliferation index (PI) was defined as the ratio of Ki-67-positive cancer cells to total cancer cells in the highest positive stain fields (at least 2,000 cells), using a microscopic grid at ×400 magnification.

Expression of NFκB, PIM-2, and DAD-1 protein in histological sections was analyzed in the smaller tissue array by immunohistochemistry, as described above, with the following antibodies: anti-NFκB (Santa Cruz Biotechnology; sc-8008; mouse monoclonal IgG; 1:10 dilution; 30' incubation time); PIM-2 (Santa Cruz Biotechnology; sc-13514; mouse monoclonal IgG; 1:10 dilution; 30' incubation time); and DAD-1 (Santa Cruz Biotechnology; sc-12173; goat polyclonal IgG; 1:10 dilution, 30' incubation time). NFκB expression was also analyzed in the large PNI array (226 patients). Cancer cells in PNI or NPNI areas were interpreted for immunoreactivity using a 0 to 3+ quantitative scoring system for both stain intensity and percentage of positive cells (labeling frequency percentage). For intensity, the grading scale ranged

<sup>4</sup> <http://www.bcm.tmc.edu/microarray>.



from no detectable signal (0) to strong signal seen at low power (3). A designation of 2 was assigned to a moderate signal seen at low to intermediate power, and a designation of 1 was assigned to a weak signal seen only at intermediate to high power.

Nuclear expression of NF $\kappa$ B was also quantified in the large PNI tissue microarray using a 0 to 3 scale. Zero correspond to no nuclear staining, 1 is faint nuclear staining, 2 is strong staining observed at medium power in <20% of the cells in the PNI cancer, and 3 is strong staining observed at medium power in >20% of the cells.

**Immunofluorescence.** Tissue culture samples were rinsed in Tris-buffered saline followed by a 60-minute incubation with primary antibodies [NF $\kappa$ B, 1:50 mouse monoclonal antibody; DAD-1, 1:50 goat polyclonal antibody, (Santa Cruz Biotechnology)]. After a second rinse, the secondary antibodies [fluorescein isothiocyanate-conjugated rabbit antimouse (1:50) and Texas red-conjugated donkey anti-goat (1:50), Zymed Laboratories] were added for 30 minutes and rinsed. 4',6-Diamidino-2-phenylindole (Vector Laboratories, Burlingame, CA) was used as a counterstain. Observation was performed using a fluorescent inverted Nikon microscope and a Q-capture imaging system.

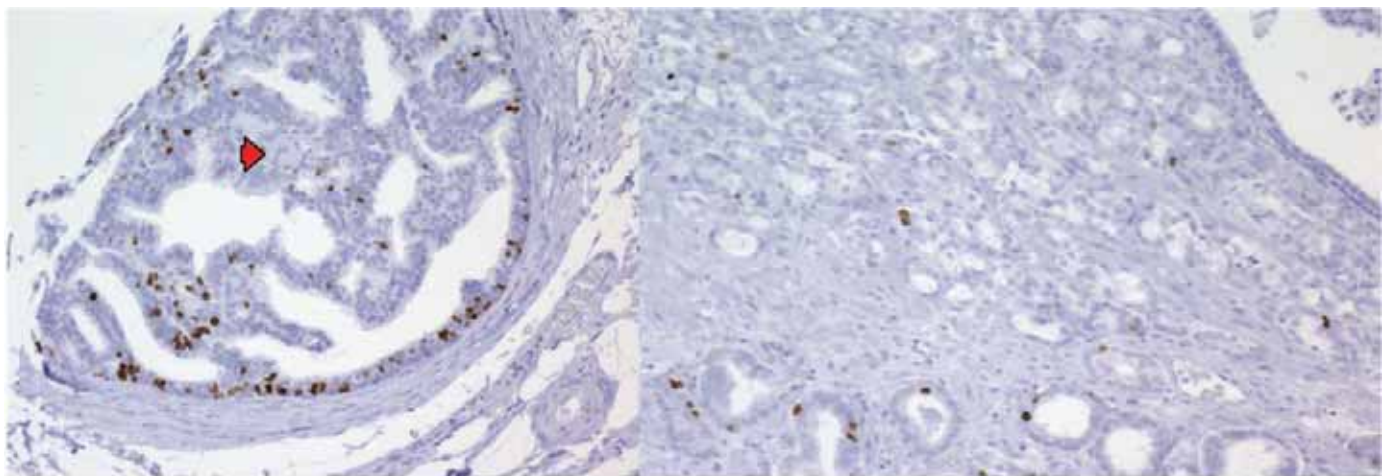
**Statistical Analysis.** Statistical analysis was conducted using Student's *t* test for analysis of significant difference between different values and was considered significant at a 95% confidence interval ( $P < 0.05$ ). The differences in NF $\kappa$ B labeling frequencies were compared between PNI cancer and NPNI specimens by using the matched pair Wilcoxon signed-rank test. The correlation of NF $\kappa$ B expression with patients' clinical and pathological variables was analyzed by the Spearman or Pearson correlation test. The predictive value of NF $\kappa$ B for recurrence-free survival was determined using the Kaplan-

Meier actuarial analysis and the log-rank test. In addition, the Cox proportional hazard regression model was used to analyze the value of using NF $\kappa$ B and other pathological and clinical markers to predict the risk of recurrence. The risk ratio and its 95% confidence interval were recorded for each marker. *P* values of <0.05 were considered statistically significant in all of our analyses. All analyses were performed with statistical software (SPSS 11.0).

## RESULTS

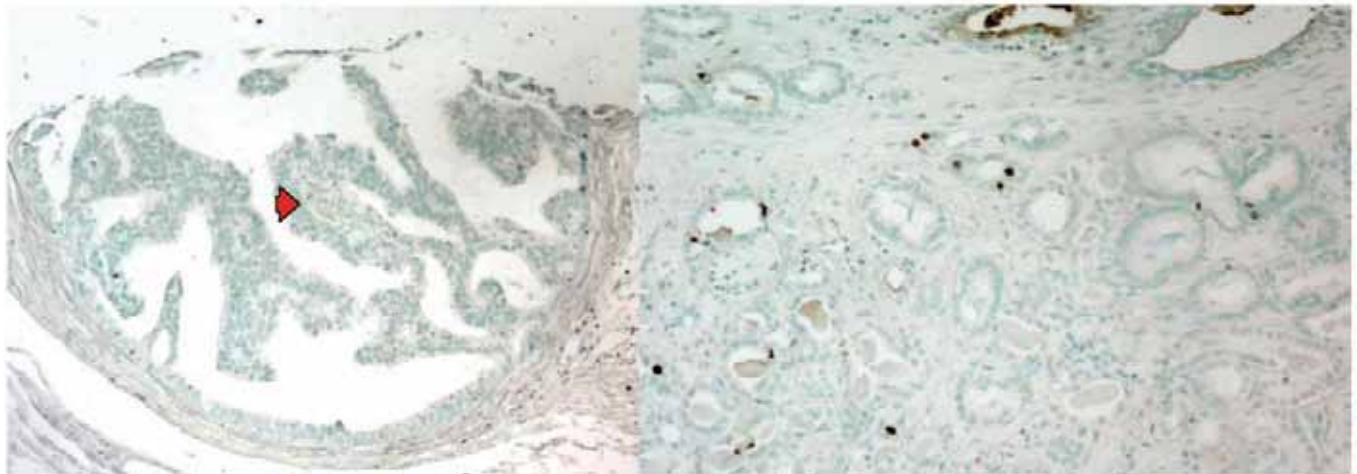
**Increased Proliferation and Reduced Apoptosis in Prostate Cancer Cells in the Perineural Space.** Matched pair analysis of the human tissue microarrays showed that prostate cancer cells associated spatially with nerves (PNI) exhibited a significant increase in PI as compared with prostate cancer cells in NPNI sites, as shown in Fig. 1. The PI in human adenocarcinoma cells at PNI sites had a mean value of  $10.25 \pm 1.2$ , whereas the PI in NPNI sites had a mean value of  $8.16 \pm 0.98$  ( $P = 0.034$ ). The AI in cancer cells at sites of PNI was significantly lower as compared with AI in prostate cancer cells not associated with PNI. The mean AI at PNI sites was  $0.68 \pm 0.16$  as compared with a mean AI of  $1.8 \pm 0.42$  at sites of cancer with no PNI ( $P = 0.010$ ; Fig. 2).

Results with the PNI *in vitro* model showed similar differences when prostate cancer cells were cocultured with dorsal root ganglion nerve tissue. Analysis of PI and AI between DU-145/DRG cocultures



Ki-67 expression in PCa in perineural invasion (100 x)

Ki-67 expression in PCa away from the nerve (100 x)



Apoptotic cells in PCa in perineural invasion (100 x)

Apoptotic cells in PCa away from the nerve (100 x)

Fig. 1. Apoptosis (TUNEL) and proliferation (Ki-67) in human prostate cancer in a perineural location and away from the nerve. Note the significant increase in proliferation and the decrease in apoptosis in the PNI cells (left panels; arrow, nerves) as compared with cancer away from the nerves (right panels).

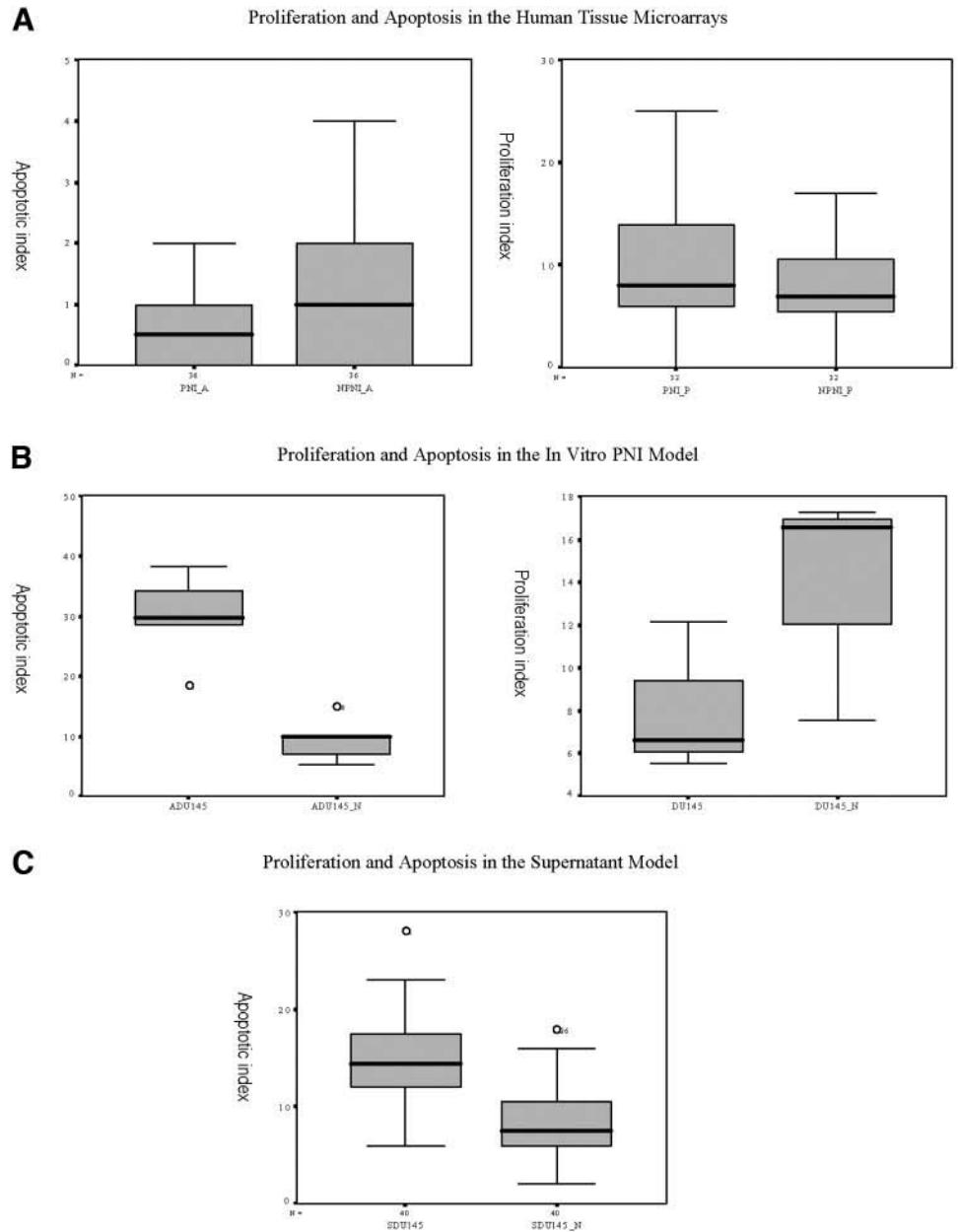


Fig. 2. *A*, AIs and PIs in human tissue microarrays. Cancer cells in the perineural location have higher PIs and lower AIs. *B*, AIs and PIs in the PNI coculture model. The model reproduces the increase in PI and decrease in AI seen in human tissues. *C*, inhibition of apoptosis is transferred by the supernatant of the coculture (DU-145+Nerve) as compared with controls.

and control DU-145 cells showed that the PI in cocultures exhibited a mean of  $9.87 \pm 2.1$  ( $n = 12$ ), whereas the mean PI in control was lower at  $6.05 \pm 2.0$  ( $n = 12$ ;  $P = 0.001$ ). The AI in the DU-145/DRG coculture was  $11.28 \pm 2.22$ , whereas the AI in control DU-145 cells was significantly higher at  $27.22 \pm 4.33$  ( $n = 12$ ;  $P = 0.004$ ; Fig. 2).

**Overexpression of Genes Related to Proliferation and Apoptosis in Prostate cancer in Perineural Location.** Profiling of genes differentially expressed in DU-145/DRG cocultures relative to DU-145 controls by gene microarray analysis showed overexpression (of at least a 3-fold differential) of 15 genes. Of these, three were known components of antiapoptosis signaling pathways. These included NF $\kappa$ B and its downstream targets PIM-2 and DAD-1. Overexpression of these factors in perineural cancer cells relative to cancer cells not associated with nerves was confirmed by quantitative PCR and showed that NF $\kappa$ B, DAD-1, and PIM-2 were each overexpressed 1.9-, 1.6-, and 2.02-fold, respectively, in DU-145/DRG cocultures as compared with DU-145 cells growing alone (Fig. 3).

Confirmation that protein was also overexpressed was shown using

immunostaining. Immunofluorescence studies with the DU-145/DRG cocultures demonstrated that NF $\kappa$ B is predominantly cytoplasmic in the DU-145 cells cultured without the nerve (control), whereas an overall increase in staining intensity and increased nuclear localization (nuclear translocation) was observed in DU-145 cells cocultured with DRG nerves in the PNI model (Fig. 4). In addition, overexpression of DAD-1 protein was evident in DU-145/DRG cocultures as compared with DU-145 controls (Fig. 4), and DAD-1 exhibited colocalization with NF $\kappa$ B in the nucleus. Immunohistochemistry for NF $\kappa$ B, DAD-1, and PIM-2 on paraffin-embedded tissues of the PNI coculture samples confirmed the quantitative PCR and immunofluorescence results (data not shown).

Examination of the human tissue microarray slides showed that the staining intensity of PIM-2 was also elevated in approximately 30% of the prostate cancer PNI sites (data not shown).

**Reversal of Perineural Invasion Antiapoptotic Effect by Genistein and BAY 11-7085.** DU-145 cells exposed to 50% (v/v) of conditioned medium derived from DU-145/DRG cocultures also

**Average Ct Value for NfκB, DAD, PIM2 and HPRT1 at different input amounts.**

Input Amount ng Total RNA	DAD-1 AverageCt	PIM-2 AverageCt	NF-κB AverageCt	HPRT1 AverageCt
200 ng	21.855±0.195	22.12±0.056	23.39±0.07	22.13±0.101
100 ng	22.305±0.064	22.5±0.045	24.31±0.044	22.865±0.13
50 ng	24.355±0.007	24.905±0.137	26.735 ± 0.345	25.375±0.05
25 ng	25.385±0.031	25.56±0.069	27.46±0.174	25.82±0.112
12.5ng	27.855±0.133	27.945±0.004	29.855±0.023	28.19±0.227
6.25 ng	29.155±0.163	29.115±0.136	30.815±0.333	29.38±0.087

Input Amount ng Total RNA	<sup>2</sup> Ct 1	<sup>2</sup> Ct 2	<sup>2</sup> Ct 3
200 ng	-0.275	-0.01	1.26
100 ng	-0.56	-0.365	1.445
50 ng	-1.02	-0.47	1.36
25 ng	-0.435	-0.26	1.67
12.5 ng	-0.335	-0.245	1.665
6.25 ng	-0.225	-0.265	1.435

The <sup>2</sup>Ct value is determined by subtracting the average HPRT1 Ct value from the average target gene value. <sup>2</sup>Ct 1 = DAD-HPRT1, <sup>2</sup>Ct 2 = NF-κB - HPRT1, <sup>2</sup>Ct 3 = PIM-2 - HPRT1

**The average Ct, <sup>2</sup>Ct results for NF-κB gene and HPRT1.**

Sample	NF-κB AverageCt	HPRT1 AverageCt	<sup>2</sup> Ct <sub>NFκB</sub>	<sup>2</sup> Ct <sub>HPRT1</sub>	Fold Difference Relative to DU-145	Fold Difference Relative to DU-145/DRG
Du-145/DRG	23.315±0.008	24.165±0.088	-0.85	-0.93	1.9053	1
DU-145	24.06 ± 0.015	23.98±0.154	0.08	0	1	
DU-145/DRG w/Genistein	22.125±0.147	22.295±0.08	-0.17	0.68		0.6242
DU-145/DRG w/BAY	26.33±0.125	26.76±0.097	-0.43	0.735		0.6008

**The average Ct, <sup>2</sup>Ct results for DAD-1 gene and HPRT1.**

Sample	DAD-1 AverageCt	HPRT1 AverageCt	<sup>2</sup> Ct <sub>DAD</sub>	<sup>2</sup> Ct <sub>HPRT1</sub>	Fold Difference Relative to DU-145	Fold Difference Relative to DU-145/DRG
Du-145/DRG	22.64±0.128	24.165±0.088	-1.525	-0.695	1.6189	1
DU-145	23.15 ± 0.115	23.98±0.154	-0.83	0	1	
DU-145/DRG w/Genistein	21.145±0.023	22.295±0.08	-1.15	0.375		0.7711
DU-145/DRG w/BAY	25.455±0.173	26.76±0.097	-1.305	0.22		0.8586

**The average Ct, <sup>2</sup>Ct results for PIM-2 gene and HPRT1.**

Sample	PIM-2 AverageCt	HPRT1 AverageCt	<sup>2</sup> Ct <sub>PIM2</sub>	<sup>2</sup> Ct <sub>HPRT1</sub>	Fold Difference Relative to Du-145	Fold Difference Relative to DU-145/DRG
Du-145/DRG	24.235±0.075	24.165±0.088	0.07	-1.015	2.0209	1
DU-145	25.065 ± 0.253	23.98±0.154	1.085	0	1	
DU-145/DRG w/Genistein	23.165±0.108	22.295±0.08	0.87	0.8		0.5744
DU-145/DRG w/BAY	27.86±0.02	26.76±0.097	1.1	1.03		0.4897

The fold difference for DAD-1, NF-κB, PIM-2 relative to HPRT1 is determined by evaluating the expression:  $2^{-\frac{2-Ct}{2-Ct_{HPRT1}}}$

Fig. 3. Quantitative PCR results of the PNI *in vitro* model. NFκB, DAD-1, and PIM-2 are increased in the coculture studies as compared with DU-145 alone. Genistein lowers NFκB and DAD-1 almost to baseline levels (left panel). BAY 11-7085 lowers NFκB, DAD-1, and PIM-2 (right panel).

showed a decrease in the AI relative to vehicle controls. There was a decrease in the mean AI in the cells cultured with PNI coculture-conditioned medium (AI = 11.02;  $n = 8$ ) compared with cells cultured with control DU-145-conditioned medium (AI = 13.52;  $n = 8$ ;  $P < 0.000$ ; Fig. 2C). The AI index showed a significant increase with the addition of genistein (AI = 17.32;  $P < 0.000$ ;  $n = 16$ ). The addition of genistein also lowered the levels of its effector targets, NFκB (0.62×), PIM-2 (0.57×), and DAD-1 (0.77×; Fig. 3). The decrease at the RNA level was translated into a decrease in protein expression as demonstrated by immunofluorescence (data not shown).

The addition of the inhibitor of IκB phosphorylation, BAY 11-7085, demonstrated similar results. In contrast to controls (DU-145 cocultured with nerves), nuclear translocation of NFκB was not identified by immunofluorescence of the PNI *in vitro* model treated with BAY 11-7085 (Fig. 5). Quantitative PCR showed a decrease in NFκB and its downstream effectors DAD-1 and PIM-2. NFκB RNA levels in BAY 11-7085-treated cells were 0.60 those of control. Similarly, DAD-1 RNA levels in BAY 11-7085-treated cells were 0.85 those of control. We also identified a decrease in PIM-2 in BAY 11-7085-treated cells (0.48) as compared with

controls (Fig. 3). More significantly, the apoptotic ratio increases in BAY 11-7085-treated cells, indicating a functional response to the IκB phosphorylation inhibition. The mean AI increase in cells treated with BAY 11-7085 was  $125.5 \pm 5.44$  ( $n = 4$ ) as compared with control DU-145-conditioned medium (AI =  $104.25 \pm 10.14$ ;  $n = 3$ ;  $P = 0.0164$ ; Fig. 5).

**Biological Significance of Nuclear Translocation of Nuclear Factor κB in Human Perineural Invasion.** Data were available in 156 patients, due to core loss and/or lack of PNI cell in the core. Overall NFκB levels were higher in the cells in PNI than in those located away from the nerve (index,  $7.18 \pm 2.39$  versus  $2.34 \pm 2.5$ ;  $P = 0.000$ ; Fig. 6B). Cytoplasmic expression of NFκB was present in all cells in PNI. Nuclear expression was identified in 72.6% of the patients (98 of 135); however, strong nuclear expression (grades 2 and 3) was present in only 38.5% and 8.1% of the patients, respectively (Fig. 6A). Strong nuclear NFκB expression in PNI correlated with other clinicopathological parameters including extracapsular extension ( $r^2 = 0.213$ ;  $P = 0.131$ ) and Gleason score ( $r^2 = 0.235$ ;  $P = 0.006$ ).

Strong levels of nuclear NFκB expression, defined as grade 2 and 3, were associated with a decrease biochemical-free survival.



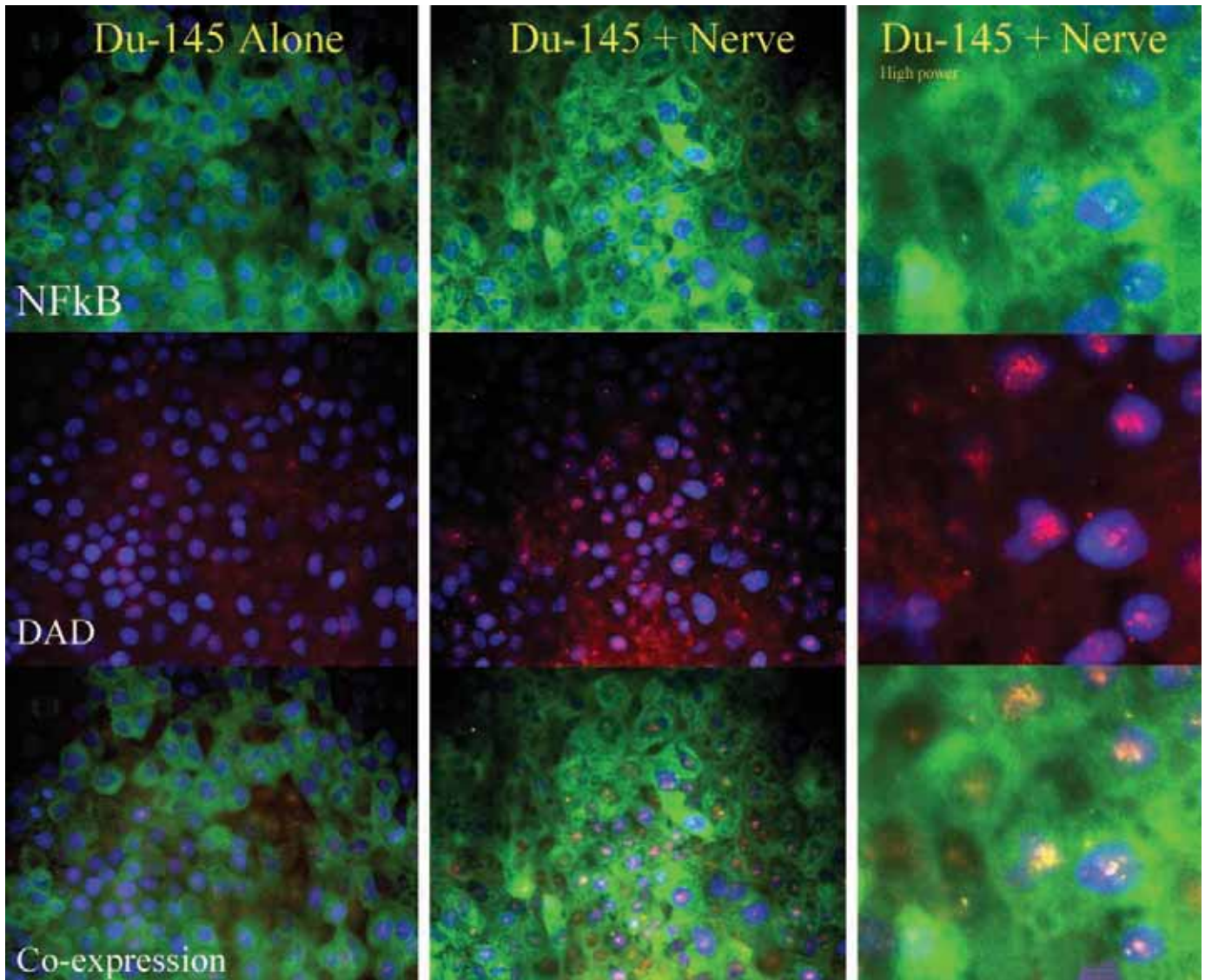


Fig. 4. *Left panels* ( $\times 100$ ) show DU-145 cells growing alone. There is cytoplasmic expression of NF $\kappa$ B (fluorescein isothiocyanate) and virtually no DAD-1 (Texas red). No coexpression is noted. The *middle panels* ( $\times 100$ ) and *right panels* ( $\times 400$ ) show the cocultures of DRG and DU-145 cells. Note the overexpression of NF $\kappa$ B with nuclear translocation [seen at higher magnification in the *right panels* ( $\times 400$ )]. Nuclear DAD-1 expression (Texas red) is increased and colocalizes to the nuclei with NF $\kappa$ B expression (yellow in the *bottom right panel*).

There was a significant difference in recurrence-free survival between cases with no expression or low expression of nuclear NF $\kappa$ B in the PNI (mean survival, 78.62 months) and those with strong expression [median survival, 67.52 months; hazard ratio = 2.053 (1.123–3.755);  $P = 0.0195$ ; Fig. 6C]. This difference was significant on univariate analysis but not on multivariate analysis.

## DISCUSSION

PNI was described as a morphological entity in the early 1900s (1). However, biological studies were never accomplished, probably due to the lack of a model. This study is the first to show biological mechanisms associated with PNI. We have demonstrated that PNI in prostate cancer resulted in inhibition of apoptosis and increased proliferation in the cancer cells associated with nerves, both in human prostate tissues and in the PNI *in vitro* model. In addition, expression of NF $\kappa$ B and its downstream effectors DAD-1 and PIM-2 was elevated in perineural cancer cells. The addition of genistein or BAY 11-7085 reversed alterations in apoptosis and lowered RNA levels of

NF $\kappa$ B, PIM-2, and DAD-1, suggesting that the NF $\kappa$ B signaling pathway regulates the alterations observed in PNI. Furthermore, nuclear translocation of NF $\kappa$ B was associated with decreased biochemical recurrence-free survival, corroborating the significance of the phenomenon in human tissues.

Neurons have numerous interactions with the epithelial and stromal components of the prostate gland. They are involved in prostate development and maintenance of histological architecture and function in the adult gland (9–14). However, the most common interaction between nerves and prostate epithelium during tumorigenesis is PNI. The biological and clinical significance of PNI in prostate cancer has been the subject of intense debate (15–18). Numerous other authors have reported varying degrees of clinical prognostic significance for PNI (15, 17, 19–23). A significant study demonstrated that the volume of tumor around the nerve, labeled as the PNI diameter, was an independent predictor of survival (24). The greater the PNI diameter, the stronger the risk of recurrence for the patient becomes. These data suggest that not all PNIs are equal and that proximity to the nerve

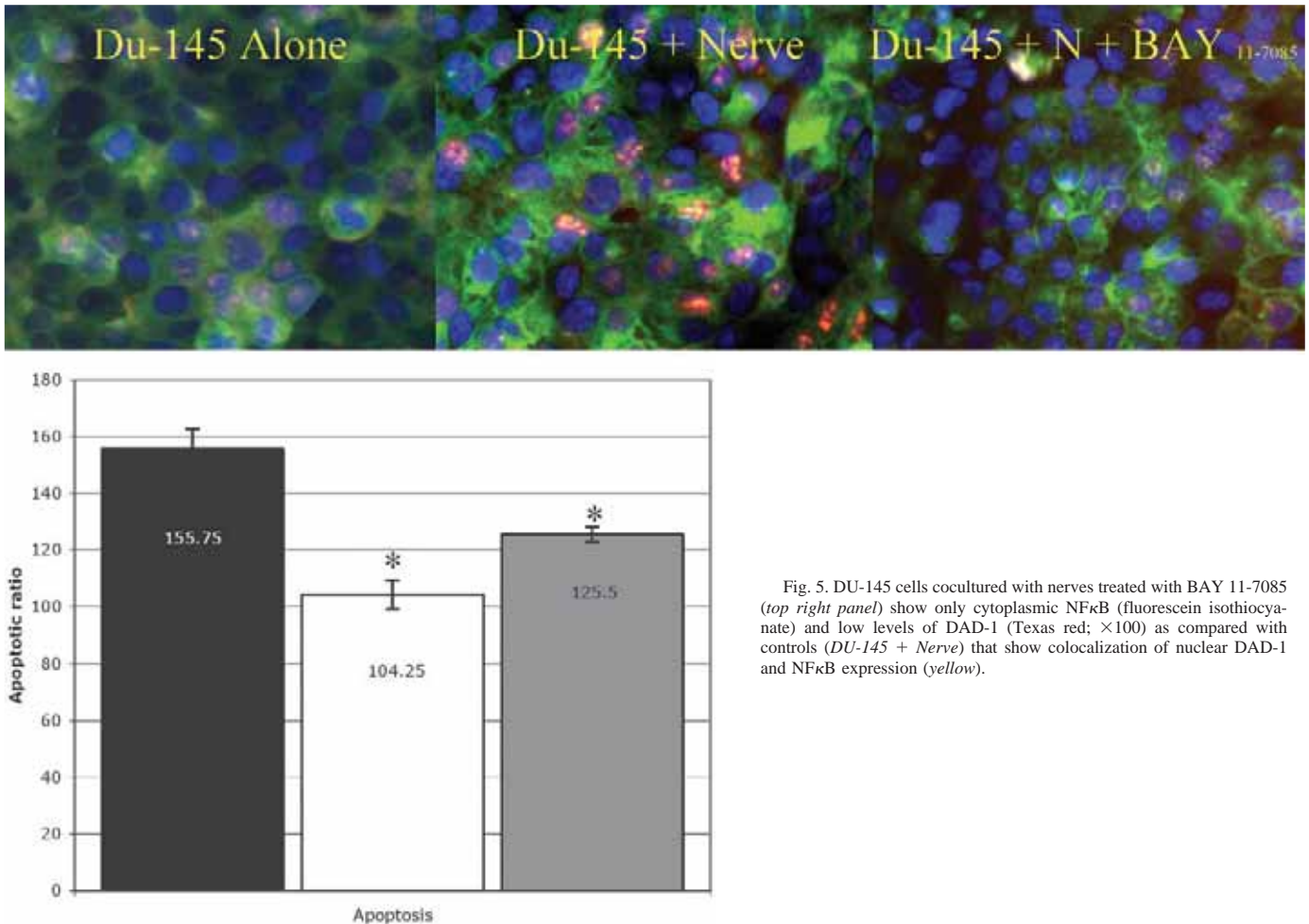


Fig. 5. DU-145 cells cocultured with nerves treated with BAY 11-7085 (top right panel) show only cytoplasmic NF $\kappa$ B (fluorescein isothiocyanate) and low levels of DAD-1 (Texas red;  $\times 100$ ) as compared with controls (DU-145 + Nerve) that show colocalization of nuclear DAD-1 and NF $\kappa$ B expression (yellow).

might provide greater growth and survival advantages in various degrees.

These studies, taken together, suggest that cancer cells in the perineural environment are influenced by the nerve to evolve a growth and survival advantage, the manifestation of which is increased tumor volume around the nerve. It follows that cancers that exploit the advantages found in the perineural microenvironment would be predicted to have a more aggressive biology and therefore the worst survival. These findings show the critical importance of studying the cancer microenvironment, including the neuroenvironment, as a key regulatory component of cancer progression. It seems likely that cancer cells have different biological abilities according to the elements that surround them. It is possible that the perineural space creates an environment that not only provides an avenue for prostate cancer invasion and spread but also creates the conditions for heightened aggressiveness that has been shown to be associated with PNI in prostate cancer. Data presented here support this hypothesis and suggest that the NF $\kappa$ B pathway is key in mediating this biology.

NF $\kappa$ B is a known regulatory element in a major survival pathway. In the present study, we demonstrate that NF $\kappa$ B is up-regulated in the PNI *in vitro* model at the RNA and protein levels. The data also strongly suggest that NF $\kappa$ B is translocated to the nuclei in prostate cancer cells in a perineural location. This process occurs in the *in vitro* PNI model as well as in human tissues. The latter is corroborated by the fact that strong nuclear NF $\kappa$ B expression in human perineural cells is associated with decreased biochemical recurrence-free survival. The lack of multivariate significance could be due to a number

of factors such as a small population and the relatively strong correlation between nuclear NF $\kappa$ B and extracapsular extension and Gleason score. More importantly, this finding is a clear demonstration that nuclear expression/translocation is clearly related to a more aggressive phenotype of prostate cancer and is a clear demonstration of the biological significance of nuclear translocation of NF $\kappa$ B in the perineural space.

PIM-2 and DAD-1 are downstream targets in the NF $\kappa$ B survival pathway (25). Both have been associated with antiapoptotic functions. Data presented here show up-regulation of these genes. Functional studies with genistein, a known inhibitor of constitutive and inducible NF $\kappa$ B activation (26, 27), and BAY 11-7085, a specific inhibitor of I $\kappa$ B phosphorylation (28), suggest that the NF $\kappa$ B and its downstream effectors are likely to be a key regulatory component in PNI. Both genistein and BAY 11-7085 seem to inhibit the up-regulation of NF $\kappa$ B as well as PIM-2 and DAD-1. Nuclear translocation seems to be inhibited and is best noted with BAY 11-7085, as would be expected with a molecule that inhibits phosphorylation of I $\kappa$ B. More importantly, the functional consequence of the activation of the NF $\kappa$ B pathway in the perineural space, inhibition of apoptosis, is partially reversed with both compounds. Accordingly, targeting the NF $\kappa$ B pathway may be a novel therapeutic approach to limit metastatic spread via PNI.

The upstream regulatory pathways that affect NF $\kappa$ B in PNI are currently unknown. Whereas neural cell adhesion molecule (NCAM) has been described in numerous cancers (29–31), we have not been able to identify NCAM in prostate cancer cells. However, nerves with



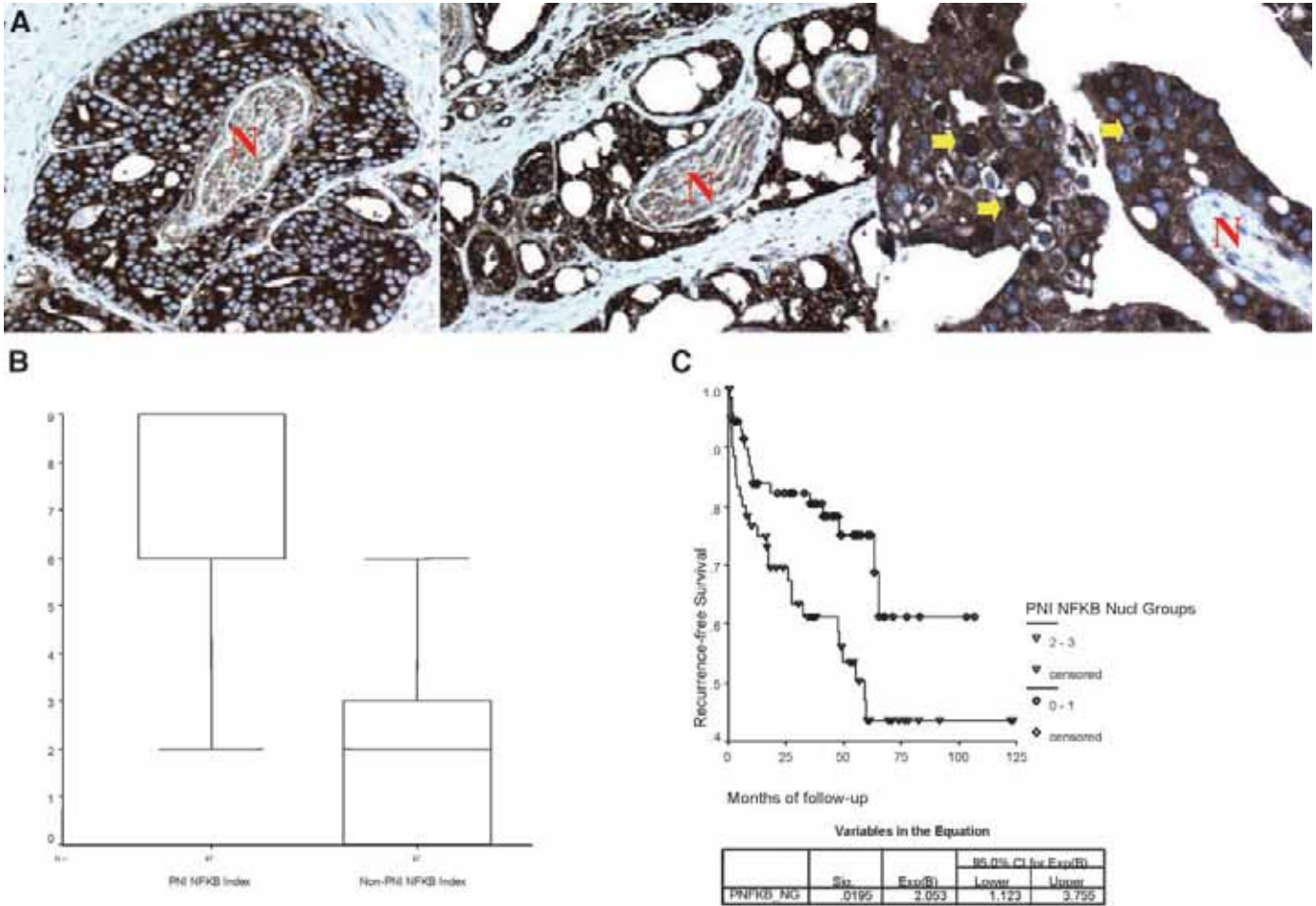


Fig. 6. A, NF $\kappa$ B expression in human tissues. Perineural prostate cancer with cytoplasmic NF $\kappa$ B expression (left panel). Nuclear and cytoplasmic expression is noted in the middle panel ( $\times 100$ ). Nuclear NF $\kappa$ B expression is indicated by the yellow arrows in the right panel ( $\times 400$ ). B, NF $\kappa$ B levels are increased in PNI as compared with cancer away from the nerve (Non-PNI). C, strong nuclear expression of NF $\kappa$ B in perineural location is associated with reduced biochemical-free survival.

prostate cancer PNI have higher levels of NCAM as compared with nerves without PNI (32). The NCAM promoter is known to be activated by neural injury, such as cancer invading the nerve. Krushel (33) demonstrated that NF $\kappa$ B-mediated transcription was increased after NCAM binding to astrocytes and neurons. NCAM homophilic binding at the cell membrane leads to increased NF $\kappa$ B binding to DNA and transcriptional activation in both neurons and astrocytes. Because NCAM and NF $\kappa$ B are present in the post-synaptic density, it is possible that higher levels of NCAM in the nerve might increase NF $\kappa$ B levels in the prostate cancer cells as they contact the nerve in PNI. This represents a potential route allowing direct communication between the cancer cells and the nerves. The relationship between NF $\kappa$ B and NCAM is bidirectional because nitric oxide also stimulates protein binding to a NF $\kappa$ B site in the promoter of the NCAM gene (34). Other potential upstream regulators are neuropeptides, which are known to be present in prostate nerves. Both bombesin (35) and dopamine (36) have been shown to stimulate NF $\kappa$ B activation.

Our studies showed that PNI is an interactive process between the cancer cells and nerves (7). In the present study, we demonstrate that this interaction likely results in growth and survival advantages for the prostate cancer cells in the perineural location and provides a putative mechanism for this phenomenon. We believe that this is the first description of a biological mechanism and functional significance associated with PNI. A more clear understanding of the specific biological mechanisms involved in PNI and the inhibition of cancer

cell apoptosis may lead to improved diagnostics/prognostics and to the development of new therapeutic strategies.

## REFERENCES

- Ernst P. Über das Wachstum und die Verbreitung Bostariger eshwulste insbesondere des Krebses in den Lymphbahnen der Nerven. *Beitr Pathol Anat* 1905;(Suppl)7:29.
- Rodin AE, Larson DL, Roberts DK. Nature of the perineural space invaded by prostatic carcinoma. *Cancer (Phila)* 1967;20:1772-9.
- Boring CC, Squires TS, Tong T, Montgomery S. Cancer statistics, 1994. *CA-Cancer J Clin* 1994;44:7-26.
- Scardino PT, Weaver R, Hudson MA. Early detection of prostate cancer. *Hum Pathol* 1992;23:211-22.
- Villers A, McNeal JE, Redwine EA, Freiha FS, Stamey TA. The role of perineural space invasion in the local spread of prostatic adenocarcinoma. *J Urol* 1989;142:763-8.
- Yang G, Wheeler TM, Kattan MW, Scardino PT, Thompson TC. Perineural invasion of prostate carcinoma cells is associated with reduced apoptotic index. *Cancer (Phila)* 1996;78:1267-71.
- Ayala GE, Wheeler TM, Shine HD, et al. In vitro dorsal root ganglia and human prostate cell line interaction: redefining perineural invasion in prostate cancer. *Prostate* 2001;49:213-23.
- Gavrieli Y, Sherman Y, Ben-Sasson SA. Identification of programmed cell death in situ via specific labeling of nuclear DNA fragmentation. *J Cell Biol* 1992;119:493-501.
- Doggweiler R, Zermann DH, Ishigooka M, Schmidt RA. Botox-induced prostatic involution. *Prostate* 1998;37:44-50.
- McVary KT, Razzaq A, Lee C, et al. Growth of the rat prostate gland is facilitated by the autonomic nervous system. *Biol Reprod* 1994;51:99-107.
- Kato T, Watanabe H, Shima M, Kaiho H. Studies on the innervation of prostate. 2. Histological changes of the dog prostate after transection of its innervating nerves [in Japanese]. *Nippon Hinyokika Gakkai Zasshi* 1971;62:704-7.

12. Watanabe H. Tissue respiration of the partially denervated dog prostate. *Tohoku J Exp Med* 1968;95:193–9.
13. Watanabe H, Shima M, Kojima M, Ohe H. Dynamic study of nervous control on prostatic contraction and fluid excretion in the dog. *J Urol* 1988;140:1567–70.
14. Watanabe H, Kato H, Kato T, Morita M, Takahashi H. Studies on the innervation of the prostate. I. Tissue respiration of the dog prostate after the cutting off of the various innervating nerves [in Japanese]. *Nippon Hinyokika Gakkai Zasshi* 1967;58:381–5.
15. de la Taille A, Katz A, Bagiella E, et al. Perineural invasion on prostate needle biopsy: an independent predictor of final pathologic stage. *Urology* 1999;54:1039–43.
16. McNeal JE, Yemoto CE. Spread of adenocarcinoma within prostatic ducts and acini. Morphologic and clinical correlations. *Am J Surg Pathol* 1996;20:802–14.
17. McNeal JE, Haillot O. Patterns of spread of adenocarcinoma in the prostate as related to cancer volume. *Prostate* 2001;49:48–57.
18. Ravery V, Boccon-Gibod LA, Meulemans A, et al. Predictive value of pathological features for progression after radical prostatectomy. *Eur Urol* 1994;26:197–201.
19. Ravery V, Boccon-Gibod LA, Dauge-Geffroy MC, et al. Role of biological and anatomo-pathologic criteria in the prognosis evaluation of patients before and after radical prostatectomy. *Prog Urol* 1994;4:673–82.
20. van den Ouden D, Kranse R, Hop WC, van der Kwast TH, Schroder FH. Microvascular invasion in prostate cancer: prognostic significance in patients treated by radical prostatectomy for clinically localized carcinoma. *Urol Int* 1998;60:17–24.
21. Anderson PR, Hanlon AL, Patchefsky A, Al-Saleem T, Hanks GE. Perineural invasion and Gleason 7–10 tumors predict increased failure in prostate cancer patients with pretreatment PSA < 10 ng/ml treated with conformal external beam radiation therapy. *Int J Radiat Oncol Biol Phys* 1998;41:1087–92.
22. Bastacky SI, Walsh PC, Epstein JI. Relationship between perineural tumor invasion on needle biopsy and radical prostatectomy capsular penetration in clinical stage B adenocarcinoma of the prostate. *Am J Surg Pathol* 1993;17:336–41.
23. McNeal JE. Cancer volume and site of origin of adenocarcinoma in the prostate: relationship to local and distant spread. *Hum Pathol* 1992;23:258–66.
24. Maru N, Ohori M, Kattan MW, Scardino PT, Wheeler TM. Prognostic significance of the diameter of perineural invasion in radical prostatectomy specimens. *Hum Pathol* 2001;32:828–33.
25. Patel NM, Nozaki S, Shortle NH, et al. Paclitaxel sensitivity of breast cancer cells with constitutively active NF-kappaB is enhanced by IkappaBalpha super-repressor and parthenolide. *Oncogene* 2000;19:4159–69.
26. Tabary O, Escotte S, Couetil JP, et al. Genistein inhibits constitutive and inducible NFkappaB activation and decreases IL-8 production by human cystic fibrosis bronchial gland cells. *Am J Pathol* 1999;155:473–81.
27. Davis JN, Kucuk O, Sarkar FH. Genistein inhibits NF-kappa B activation in prostate cancer cells. *Nutr Cancer* 1999;35:167–74.
28. Ni H, Ergin M, Huang Q, et al. Analysis of expression of nuclear factor kappa B (NF-kappa B) in multiple myeloma: downregulation of NF-kappa B induces apoptosis. *Br J Haematol* 2001;115:279–86.
29. Hutcheson JA, Vural E, Korourian S, Hanna E. Neural cell adhesion molecule expression in adenoid cystic carcinoma of the head and neck. *Laryngoscope* 2000;110:946–8.
30. Kenmotsu M, Gouchi A, Maruo Y, et al. The expression of neural cell adhesion molecule (NCAM), neural invasion and recurrence patterns in rectal cancer: a study using anti-NACM (neural cell adhesion molecule) antibody [in Japanese]. *Nippon Geka Gakkai Zasshi* 1994;95:66–70.
31. Seki H, Koyama K, Tanaka J, Sato Y, Umezawa A. Neural cell adhesion molecule and perineural invasion in gallbladder cancer. *J Surg Oncol* 1995;58:97–100.
32. Li R, Wheeler T, Dai H, Ayala G. Neural cell adhesion molecule is upregulated in nerves with prostate cancer invasion. *Hum Pathol* 2003;34:457–61.
33. Krushel LA, Cunningham BA, Edelman GM, Crossin KL. NF-kappaB activity is induced by neural cell adhesion molecule binding to neurons and astrocytes. *J Biol Chem* 1999;274:2432–9.
34. Simpson CS, Morris BJ. Regulation of neuronal cell adhesion molecule expression by NF-kappa B. *J Biol Chem* 2000;275:16879–84.
35. Levine L, Lucci JA III, Pazdrak B, et al. Bombesin stimulates nuclear factor kappa B activation and expression of proangiogenic factors in prostate cancer cells. *Cancer Res* 2003;63:3495–502.
36. Takeuchi Y, Fukunaga K. Differential regulation of NF-kappaB, SRE and CRE by dopamine D1 and D2 receptors in transfected NG108–15 cells. *J Neurochem* 2003;85:729–39.